12-GHz-Band FM Receiver for Satellite Broadcasting

YOSHIHIRO KONISHI, SENIOR MEMBER, IEEE

Abstract—**This paper describes the low-noise low-cost receiver for satellite broadcasting with new technology developed by us. The paper also describes the image recovery theory, the design principle of our downconverter, a frequency-stabilized local oscillator with bipolar transistors, the required limiting factor of a limiter, the removing circuit of an energy dispersal signal [1], and a parabolic antenna for circularly polarized waves together with the performance of our device. The experimental results obtained through the Communication Technology Satellite (CTS) are also shown.**

I. Introduction

THE LOW-NOISE low-cost receiver is needed for a ground station for satellite broadcasting. A SHF-FM receiver usually has a configuration as shown in Fig. 1. The system shown in Fig. 1(a) can supply n output channels which are available, for example, for a CATV system. On the other hand, the system shown in Fig. 1(b) can be used for selecting one channel from n channels by changing the local oscillator frequency used for a second converter C_2. This will be preferable for a direct home receiving system in the case of future satellite broadcasting.

In Fig. 1 the preamplifier (PA) has a low-noise figure. A parametric amplifier, a field effect transistor amplifier (FET), or a tunnel diode amplifier (TDA) can be used. Image recovery techniques, however, have recently permitted one to significantly reduce the noise figure of SHF downconverters. A preamplifier is unnecessary in this case as shown by the dotted line in Fig. 1, except in the case of an extremely low-noise receiver. To achieve such a low-noise receiver without a preamplifier, we propose the use of a planar low-noise downconverter circuit mounted in waveguide. This technique permits us to achieve low-noise performance and low-production cost.

The paper presents the image recovery theory with the parametric effect of a mixer diode taken into consideration, the construction and design principle of the downconverter, and, lastly, the newly developed low-cost frequency-stabilized local oscillator with 10^{-7} ppm used with our downconverter. The IF circuit, the selection of the frequency band, and the limiting factor required especially for FM improvement are described. The experimental circuit made to remove an energy dispersal signal is also presented. The parabolic receiving antenna, either for circularly or linearly polarized waves, is available and it is described together with its performance. Lastly, the author's approach to low cost is discussed from the newly developed technology and the manufacturing process point of view.

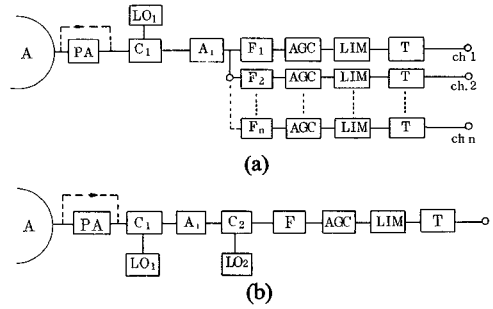

A : Receiving antenna
PA : Preamplifier
C_1 : SHF down-converter
A_i : IF amplifier
F_i : IF bandpass filter
AGC : Automatic gain control
LIM : Limiter
T : Signal processing circuit
LO_1 : Local oscillator used for SHF down converter
LO_2 : Local oscillator used for 2nd converter

Fig. 1. Block diagram of SHF-FM receiver.

II. Downconverter

A. Consideration on the Image Recovery Technique

A low-noise downconverter using the image recovery technique must be designed such that it operates under the optimum reactive load viewed from the mixer diode at the image frequency. The parametric effect caused by the junction capacitance of a mixer diode is most important to determine the appropriate operation of the image recovery downconverter as described in the following.

Since a mixer diode has the equivalent circuit shown in Fig. 2, the operation of the downconverter can be described by the equivalent networks shown in Fig. 3 and

Manuscript received November 3, 1978.
The author is with NHK Technical Research Laboratories (Japan Broadcasting Corporation), Tokyo 157, Japan.

0018-9480/78/1000-0720$00.75

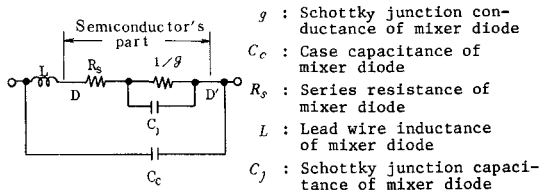

Fig. 2. Equivalent circuit of mixer diode.

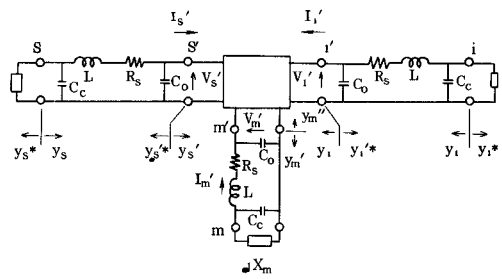

Fig. 3. Equivalent network of a downconverter taking L, C_c, R_s, and junction capacitance into account.

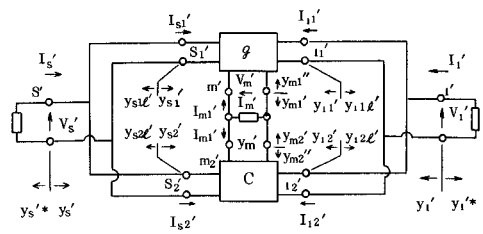

Fig. 4. Equivalent network of the range between terminals S' and i' in Fig. 2.

Fig. 4, where the g and c circuit take the matrix forms $[g]$ and $[c]$ of (1):

$$[g]=\begin{bmatrix} g_0 & g_p & g_{2p} \\ g_p & g_0 & g_p \\ g_{2p} & g_p & g_0 \end{bmatrix}$$

$$[c]=\begin{bmatrix} 0 & j\omega_s c_p & j\omega_s c_{2p} \\ j\omega_i c_p & 0 & j\omega_i c_p \\ -j\omega_m c_{2p} & -j\omega_m c_p & 0 \end{bmatrix} \cdot \quad (1)$$

In (1), g_{np} $(n=0,1,2)$ and c_{np} $(n=0,1,2)$ are the Fourier expanded nth term of a periodically variable junction conductance g and capacitance C of a mixer diode excited by a local oscillator.

The conversion loss L_c between terminals S and i in Fig. 3 can be expressed by (2):

$$L_c = L_1 L_c' L_2$$

$$L_1 = 1 + \frac{R_s|y_s'+j\omega_s c_0|^2}{\mathrm{Re}\cdot(y_s')}$$

$$L_2 = 1 + R_s\left|\frac{y_i'^*-j\omega_i c_0}{1-R_s y_i'^*+j\omega_i c_0 R_s}\right|^2 \Big/ \mathrm{Re}\cdot\left(\frac{y_i'^*-j\omega_i c_0}{1-R_s y_i'^*+j\omega_i c_0 R_s}\right)$$

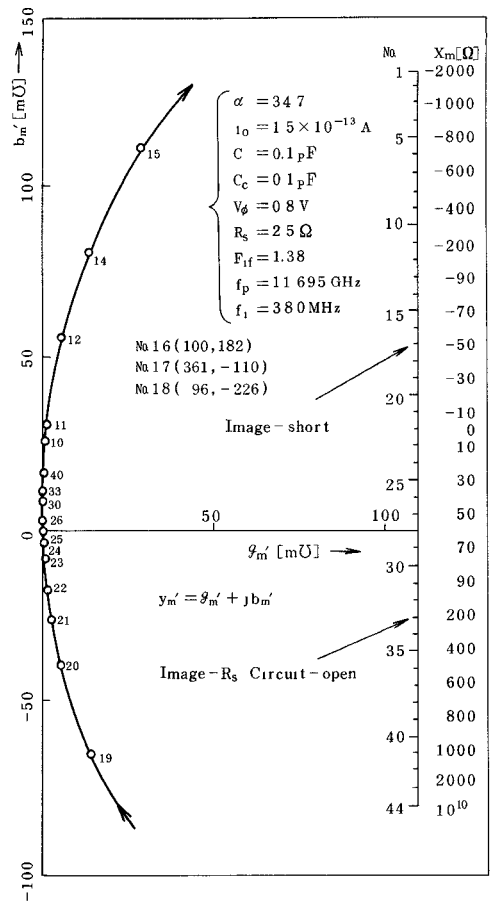

Fig. 5. Relation between y_m' and X_m.

$$L_c' = \frac{|Y_{si}'|^2}{|y_s'-Y_{ss}'|^2}\cdot\frac{\mathrm{Re}\cdot(y_s')}{\mathrm{Re}\cdot(y_i')}$$

$$Y_{ss}' = g_0 - \frac{(g_{2p}+j\omega_s c_{2p})(g_{2p}-j\omega_m c_{2p})}{g_0+y_m'^*}$$

$$Y_{si}' = g_p + j\omega_s c_p - \frac{(g_{2p}+j\omega_s c_{2p})(g_p-j\omega_m c_{2p})}{g_0+y_m'^*}. \quad (2)$$

In (2), L_1 is the transmission loss caused by R_s, where Re· means the real part in the signal path and L_2 the loss in the IF circuit, respectively. L_c' is the conversion loss of the diode junction. Equation (2) indicates that L_c changes with the admittance y_m' viewed from the diode junction at the image frequency. Since y_m' is a function of the load reactance X_m connected to the diode, L_c can be obtained as a function of X_m as shown in Fig. 5. In Fig. 5, the axis labeled No. 1–44 means the situations where X_m takes the corresponding values described at the right-hand side of this figure. g_m' and b_m' are the real and imaginary parts of y_m' shown in Fig. 3, F_{IF} the preamplifier noise figure, f_p the pumping frequency, and f_i the intermediate frequency. The computed results are shown in Fig. 6.

At No. 33 (image-open), L_c has a minimum because of the parametric effect of the junction capacitance C_j. But L_1 has a large value, because the matched signal impedance becomes low.

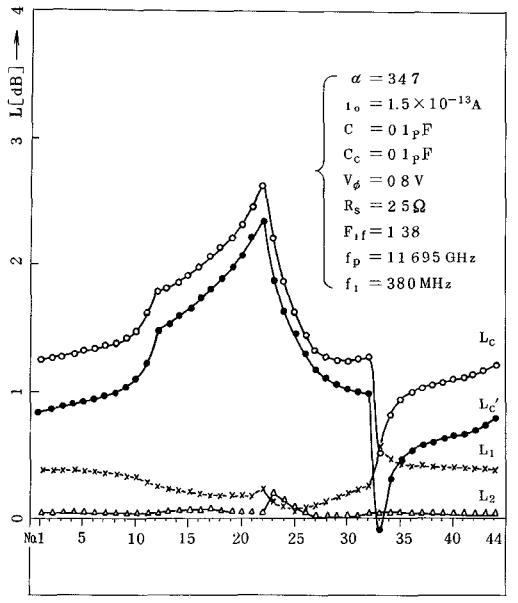

Fig. 6. Computed conversion loss.

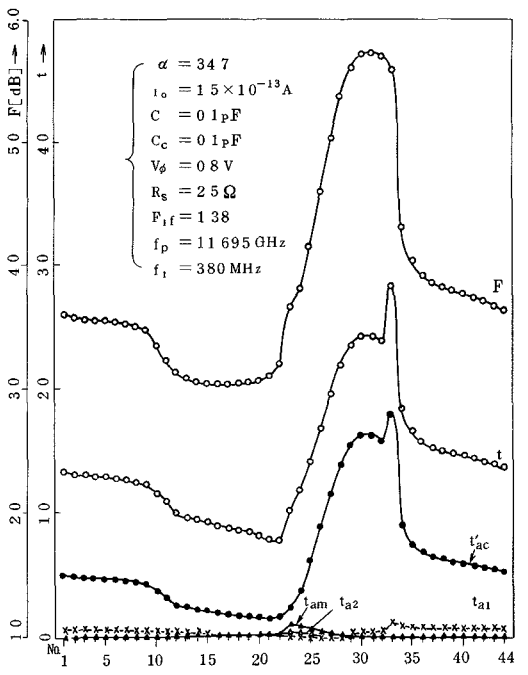

Fig. 7. Noise temperature ratio and noise figure.

At No. 17 (image-short), the effect of C_j can be neglected; therefore, the value of L_c is almost the same as that without C_j.

Next, the relation between the conversion loss and the noise performance must be considered. By denoting noise temperature ratios corresponding to the thermal noise generated at R_s in the signal, IF and image circuits as t_{a1}, t_{a2}, and t_{am}, respectively, these values can be obtained by (3), (4), and (5) deduced from Fig. 3. The calculated values are also shown in Fig. 7.

$$t_{a1}=\frac{1}{L_c'L_2}\left(1-\frac{1}{L_1}\right) \tag{3}$$

$$t_{a2}=1-\frac{1}{L_2} \tag{4}$$

$$t_{am}=4R_s\left|\frac{y_m'-j\omega_m c_0}{y_m'+y_m''}\right|\cdot|A_{im}|^2\cdot g_i'\cdot\frac{1}{L_2} \tag{5}$$

where

$$A_{im}=\frac{(g_{2p}+j\omega_s c_{2p})(g_p+j\omega_i c_p)-(g_p+j\omega_i c_p)(g_0+y_s'^*)}{(g_0+y_s'^*)(g_0+y_i'^*)-(g_p+j\omega_i c_p)(g_p+j\omega_s c_p)}.$$

The value of t_{am} becomes large near No. 24 because the admittance at the image terminal m' is reduced by the parallel resonance at this point, which results in generation of a maximum thermal noise. The situation is shown in Fig. 7 (t_{am}).

The shot noise generated in the g circuit of Fig. 4 appears at the signal, IF, and image terminal with the values of N_s, N_i, and N_m, respectively. The shot noises N_i, N_s, and, N_m arrive at the IF load $y_i'^*$ through the paths as shown in Figs. 8(a), (b), and (c), respectively. Taking these paths into consideration, we obtain, in (6), the noise temperature ratio t_{ac}' caused by shot noise.

The computed result of t_{ac}' is shown in Fig. 7, and the physical meaning of the performance of t_{ac}' can be explained as follows.

The input admittance of the C circuit of Fig. 3 viewed from the IF terminal is much smaller than $y_i'^*$ through the points of No. 1–44 except the point near No. 33. At point No. 33, the C circuit which operates as an upconverter where the noise N_i is amplified through the C circuit, arrives again at terminal S_1' and is transformed to an IF noise. Thus t_{ac}' becomes the maximum values at the point near No. 33.

$$t_{ac}'=\frac{ng_i'|A|^2}{L_2}\left(\frac{|B_i|}{g_{i1l}'}+\frac{|B_s\|A_3|^2}{g_{s1l}'}\cdot\left|\frac{y_{s1l}'}{y_{i1l}'}\right|^2+\frac{|B_m\|A_4|^2}{g_{m1}'}\cdot\left|\frac{y_{m1}'}{y_{i1l}'}\right|^2\right)$$

$$B_i=\frac{1}{L_{i1,\mathrm{out}}}-\frac{1}{L_{s1,\mathrm{in}}\cdot L_{gsi}'}-\frac{1}{L_{m1,\mathrm{in}}\cdot L_{gmi}'}$$

$$B_s=\frac{1}{L_{s1,\mathrm{out}}}-\frac{1}{L_{i1,\mathrm{in}}\cdot L_{gis}'}-\frac{1}{L_{m1,\mathrm{in}}\cdot L_{gms}'}$$

$$B_m=\frac{1}{L_{m1,\mathrm{fout}}}-\frac{1}{L_{s1,\mathrm{in}}\cdot L_{gsm}'}-\frac{1}{L_{i1,\mathrm{in}}\cdot L_{gim}'}$$

$$A=1/(1-A_1-A_2)$$

$$A_1=\frac{\beta_{igc}\alpha_{cis}\beta_{scg}\alpha_{gsi}}{1-\beta_{scg}\alpha_{gsm}\beta_{mgc}^*\alpha_{cms}}$$

$$A_2=\frac{\beta_{igc}\alpha_{cim}\beta_{mcg}^*\alpha_{gmi}}{1-\beta_{sgc}\alpha_{csm}\beta_{mcg}^*\alpha_{gms}}$$

$$A_3=\frac{\beta_{sgc}\alpha_{csm}\beta_{mcg}^*\alpha_{gmi}}{1-\beta_{sgc}\alpha_{gms}\beta_{mcg}^*\alpha_{csm}}$$

$$A_4=\frac{\beta_{mgc}^*\alpha_{cms}\beta_{scg}\alpha_{gsi}}{1-\beta_{scg}\alpha_{cms}\beta_{mgc}^*\alpha_{gsm}} \tag{6}$$

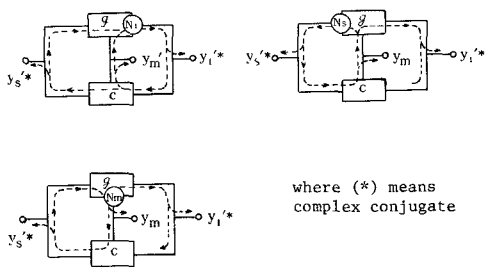

Fig. 8. Path which shot noise takes to arrive at the IF terminal.

where $L_{i1,\text{out}}$, $L_{s1,\text{out}}$, $L_{m1,\text{out}}$ are mismatch losses at i_1, s_1, m_1 terminals when the power flows out from the g circuit, $L_{i1,\text{in}}$, $L_{s1,\text{in}}$, $L_{m1,\text{in}}$ are mismatch losses when the power flows into the g circuit, and L'_{gsi}, L'_{gis}, L'_{gim}, L'_{gmi}, L'_{gsm}, L'_{gms} are conversion losses at $s'_1 \rightarrow i'_1$, $i'_1 \rightarrow s'_1$, $i'_1 \rightarrow m'_1$, $m'_1 \rightarrow i'_1$, $s'_1 \rightarrow m'_1$, and $m'_1 \rightarrow s'_1$, respectively, $\alpha_{gsi} = -I'_{i1}/I'_{s1}$,

$$\alpha_{gsm} = -I'^{*}_{m1}/I'_{s1}, \qquad \alpha_{gms} = -I'_{s1}/I'^{*}_{m1},$$
$$\alpha_{gmi} = -I'_{i1}/I'^{*}_{m1}, \qquad \alpha_{csm} = -I'^{*}_{m2}/I'_{s2},$$
$$\alpha_{cms} = -I'_{s2}/I'^{*}_{m2}, \qquad \alpha_{cis} = -I'_{s2}/I'_{i2},$$
$$\alpha_{cim} = -I'^{*}_{m2}/I'_{i2}, \qquad \beta_{igc} = y'_{i2}/y'_{s1l},$$
$$\beta_{sgc} = y'_{s2}/y'_{s1l}, \qquad \beta_{scg} = y'_{s1}/y'_{s2l}, \qquad \beta_{mgc} = y''_{m2}/y'_{m1},$$
$$\beta_{mcg} = y''_{m1}/y'_{m2}, \qquad y'_{s1l} = g'_{s1l} + jb'_{s1l},$$
$$y'_{i1l} = g'_{i1l} + jb'_{i1l}, \text{ and } \quad y'_{m1} = g'_{m1} + jb'_{m1}.$$

The total noise temperature ratio takes the values of (7):

$$t = \frac{1}{L_c} + t_{a1} + t_{a2} + t_{am} + t'_{ac}. \tag{7}$$

The noise figure of the downconverter can be obtained by (8):

$$F = L_c(t + F_{\text{IF}} - 1). \tag{8}$$

In (8), F_{IF} is the noise figure of the IF amplifier connected to the downconverter. The computed values of F are shown in Fig. 7.

As illustrated by Fig. 7, F is large in the range between No. 24 and 35. This is caused by the large value of t'_{ac} as described above. Another reason is that the conversion loss L_c and noise temperature ratio t_{am} become large because of the large resistive load, which results in deteriorating L_c and t_{am}. For the above reasons, it is preferable to operate the converter under the image short condition.

B. Downconverter Constructed with a Planar Circuit Mounted in Waveguide

The construction and the fundamental design concept will be described in this section. The new technology developed by the author, a planar circuit mounted in waveguide (PCMW) [2], is used in this downconverter. The converter has a planar circuit sandwiched in a waveguide. On the planar circuit, proper patterns required for the function of the downconverter are made by etching or

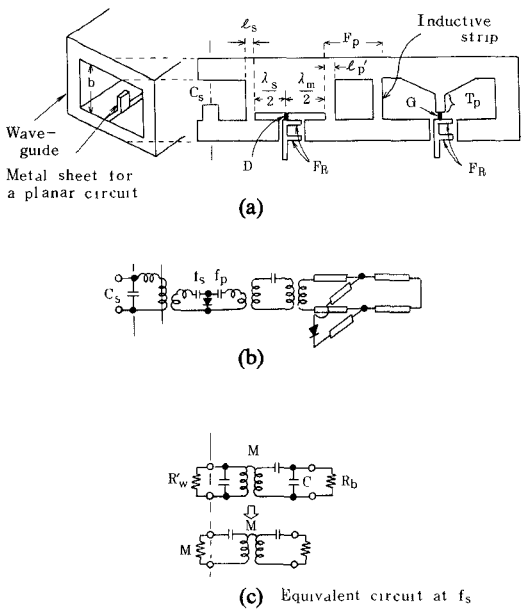

Fig. 9. Example of the construction of 12-GHz downconverter with planarcircuit mounted in waveguide.

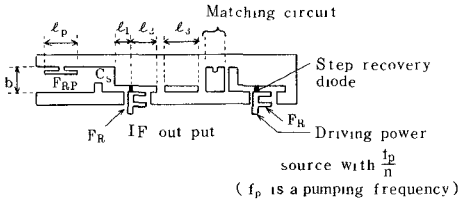

Fig. 10. Another example of a planar circuit.

punching technology. Examples of the construction [2] and the equivalent network are shown in Fig. 9, and in Fig. 10. In Fig. 9, D is a Schottky mixer diode and G is a Gunn diode. In Fig. 10, l_2 is used to realize the image short condition for the reason mentioned in 2.1. l_1 and C_s match the diode impedance to a waveguide. F_R not only rejects the local oscillator power but also permits it to supply the local and signal power to the mixer diode. The planar circuit is designed by using equivalent networks of several discrete parts as shown in Fig. 11. The network elements were obtained theoretically [2] or empirically. For example, the elements of Fig. 11(e) were reported in [3]. The effective length Δl is obtained by a variational method, and the result is expressed by (9a) and (9b):

$$\Delta l = \frac{\lambda_s \omega \mu_0 \sum_{n=1}^{\infty} \frac{1}{\gamma_n^{(2)}} \langle \bar{e}_{nt}^{(2)} \times \bar{h}_{1t} \rangle^2}{2\pi Z_0} \tag{9a}$$

where

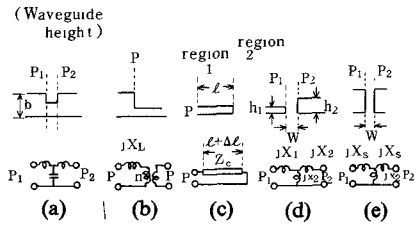

Fig. 11. Equivalent networks of discontinuity of a planar circuit mounted in a waveguide.

$$Z_c = \frac{120\pi}{\sqrt{1-\left(\frac{\lambda_0}{\lambda_c}\right)^2}} \quad \text{and} \quad \lambda_s = \frac{\lambda_0}{\sqrt{1-\left(\frac{\lambda_0}{\lambda_c}\right)^2}} \tag{9b}$$

where

λ_0 free space wavelength,
$\gamma_n^{(2)}$ propagation constant of nth mode in the cutoff waveguide of region 2 in Fig. 11(c),
λ_c cutoff wavelength in ridge waveguide,
$\bar{e}_{nt}^{(2)}$ normalized transversal electrical field in the cutoff waveguide of region 2 in Fig. 11(c),
$\bar{h}_{1t}$ normalized transversal dominant magnetic field in the ridge guide.

$$\iint_{s_2} |e_{nt}^{(2)}|^2 ds = 1 \qquad \iint_{s_1} |h_{1t}|^2 ds = 1$$

where s_1; s_2 are the sectional areas in regions 1 and 2. Network elements of Figs. 11(a), (b), and (d) were obtained by empirical methods.

C. Local Oscillator Used for the Downconverter

A local oscillator is usually obtained by using a Gunn diode or by using a step recovery diode. The Gunn oscillator should be locked by a resonator such as a dielectric resonator to stabilize the frequency. With this technique, the frequency deviation can be kept within 150 kHz for the temperature fluctuation from -30–$+60$°C. The step recovery diode is excited by a UHF source which is obtained by multiplying a crystal oscillator. The latter method should be considered in the future for a low-cost approach.

Recently, we have developed a temperature stabilized L-band oscillator by using bipolar transistors and a dielectric resonator, which is used for driving a step recovery diode to multiply four times. The schematic diagram is shown in Fig. 12. The frequency deviation is less than 100 kHz at X band over the range of -20–$+40$°C. The dielectric resonator is used as a narrow bandpass filter inserted in a feedback loop of the transistor amplifier. This stable oscillator has a performance which is quite suitable for low-cost mass production, and it will be one solution for a low-cost and stable oscillator.

III. IF Amplifier and Limiter

The frequency band of an IF amplifier should be chosen taking into consideration the bandwidth to be converted, the required noise figure, protection from other

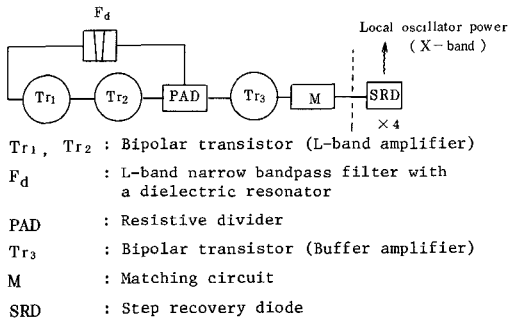

Fig. 12. Stabilized local oscillator using bipolar transistors and SRD.

terrestrial waves such as VHF, and UHF bands, image frequency problem, and the distance between an outdoor unit and an indoor unit. If the required bandwidth is resonably narrow as about 200 MHz, f_i can be chosen between the VHF-TV band and UHF-TV band. In this case, the noise figure of the IF amplifier is less than 1.5 dB, and the cost can be made low in wideband gain matching operation.

If the required bandwidth is wider than 500 MHz, f_i might be chosen at the frequency range of 1 GHz. In this case, the noise figure of the IF amplifier is less than 2.0 dB in wideband gain matching operation.

For a limiter of a satellite broadcasting receiver, operation with weak signals is quite important, because in rain the receiver operates around the threshold level. If the operation of the limiter is not sufficient, the AM components of noise are detected, resulting in the deterioration of signal-to-noise ratio. Qualitative deterioration can be obtained from (10).

$$\frac{[SN]_0}{[SN]} = 1 + \frac{3\Delta f_m^2}{4 f_h^2 A^2} \tag{10}$$

where

A AM compression (for example, $A=10$ for 20-dB compression)
$[SN]_0$ signal-to-noise ratio of detected video signal for the case of ideal limiter where, $A=\infty$
$[SN]$ signal-to-noise ratio for the case of a practical limiter, where A takes finite values
Δf_m peak-to-peak frequency deviation
f_h highest video frequency.

For example, when $\Delta f_m = 12$ MHz and $f_h = 4.2$ MHz, the deterioration of the signal-to-noise ratio takes the values as shown in Table I. For the above reason, it is preferable to design a limiter having AM suppression of more than 25 dB. PM–AM conversion is another important factor to avoid the deterioration of the signal-to-noise ratio which takes place inside the IF amplifier. It should be taken into consideration in designing the limiter.

The performance of the IF bandpass filters ($F_1, \cdots, F_n, F$) shown in Fig. 1 should be specified considering spectrum distribution, phase distortion, and channel separation. For the phase distortion, the surface acoustic

TABLE I
LIM (dB) = $10 \log_{10} A^2$

LIM [dB]	$\frac{[SN]_0}{[SN]}$	$10 \log_{10} \frac{[SN]_0}{[SN]}$
10	1613	2074 [dB]
20	10613	0.258 [dB]
30	100613	0.0265 [dB]

TABLE II
MEASURED VALUES AT 12 GHz

item \ diameter	0.6 m	1.0 m	1.6 m
G [dB]	34.9	39.6	43.9
η	0.54	0.63	0.64

wave filter will be preferable in the future, since it has linear phase performance.

IV. Signal Processing Circuit

An FM signal appearing at the output of the limiter is usually transformed to video and sound signals by a normal discriminator. To get an AM signal available for a domestic TV receiver, video and sound signals should be remodulated, respectively, and they must be combined. Recently, a new technique, the FM–AM direct converter, has been developed. This is reported in [4]. In this circuit, it is not necessary to use a discriminator and remodulators, bringing about a simple- and low-cost construction. But, with this circuit, the sound subcarrier level becomes lower, requiring an additional amplifier for the sound subcarrier, and some technology available to energy dispersal signal must be developed in the future.

To remove the energy dispersal signal [1], we are using a rather high speed peak clamping circuit, in which clamping the vertical synchronous period is skipped to avoid distortion caused by the small time constant of the clamping circuit. The energy dispersal signal can be decreased by means of such a peak clamping method; −30 dB at 15 Hz and −20 dB at 20 Hz. The circuit operates quite effectively even under a threshold level.

V. Antenna

A receiving antenna for satellite broadcasting should have high gain, high efficiency, and low cost. Therefore, parabolic antennas are made in aluminum, fiber reinforced plastic, and sometimes mesh. The practical values of antenna gain G and efficiency η are shown in Table II.

VI. Practical Performance of the Receiver Developed by NHK and its Experimental Results

The 12-GHz SHF receiver, developed by NHK, uses a planar circuit mounted in waveguide and the its performance is shown in Figs. 13(a) and (b). Experimental values of L_c and F are a little larger than calculated ones shown in Figs. 6 and 7. This difference is caused by the

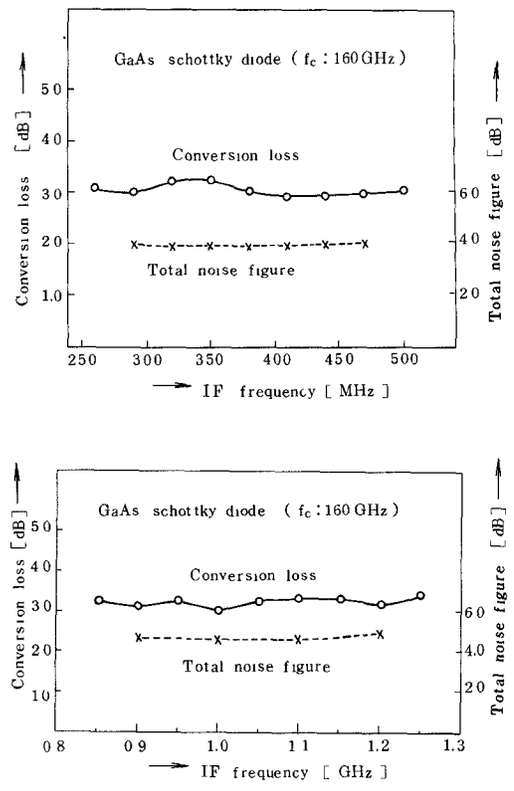

Fig. 13. Performance of a 12-GHz downconverter with planar circuit mounted in waveguide.

mismatching loss between the converter and the preamplifier, and the RF circuit loss. The receiver was used to receive the signal from CTS in the U.S.A. This experiment was made under the joint experiment "Advanced Ground Receiving Equipment (AGREE)"[1] between NASA and NHK. In this experiment, we have received the signal with the weighted signal-to-noise ratio of 49.5 dB and 45 dB by using 1- and 0.6-m antennas under the condition of EIRP of 58.5 dBW.

For the reception of circularly polarized waves, a polarizer is connected to the top of a primary radiator. Such an antenna has more than 25-dB depolarization and less than 0.2-dB loss of antenna gain. With this antenna, either the circularly or linearly polarized wave can be received only by rotating the polarizer around the axis of the primary radiator.

References

[1] I.T.U.: Final acts of the W.A.R.C. for the planning of the B.S.S. in frequency band 11.7–12.2 GHz (regions 2 and 3) and 11.7–12.5 GHz (in region 1), Geneva 1977.
[2] Y. Konishi, *et al.*, "The design of planar circuit mounted n waveguide and the application to low noise 12 GHz converter," presented at IEEE S-MTT Int. Microwave Symp., June 12–14, 1974.
[3] ——, "The design of a bandpass filter with inductive strip—Planar circuit mounted in waveguide," *IEEE Trans.* Microwave Theory Tech., vol. MTT-22, pp. 869–873, Oct. 1974.
[4] Y. Konishi, "Proposed SHF FM receiver for satellite broadcasting," in *Proc. IEEE Int. Conf. Communications*, pp. 36-15–36-19, 1973.

[1]This is a joint experiment by NASA and the Technical Research Laboratories of Nippon Hoso Kyokai (NHK), Japan. The participation of NHK is being sponsored by the Radio Research Laboratories of the Ministry of Posts and Telecommunications, Japan.